VOL. 20, NO. 20, OCTOBER 2025 ISSN 1819-6608
ARPN Journal of Engineering and Applied Sciences

www.arpnjournals.com

IMPACT OF INADEQUATE CONFINEMENT IN RC COLUMNS OF BUILDINGS UNDER THE UPDATED INDONESIAN SEISMIC CODE ON STRUCTURAL PERFORMANCE

Fajri Yusmar, Nevy Sandra, Eka Juliafad, Prima Zola, Nidal Zuwida, and Laras Oktavia Andreas
Department of Civil Engineering, Faculty of Engineering, Padang State University, Indonesia
E-Mail: fajriyusmar@ft.unp.ac.id

ABSTRACT

The vulnerability of reinforced concrete buildings in Indonesia-especially in seismic regions like Padang-has been worsened by poor detailing and outdated codes. This study evaluates the seismic performance of a four-story office building designed initially under SNI 1726:2012 and SNI 2847:2013, considering the updated seismic demands in SNI 1726:2019. Linear analysis showed that several beams no longer met strength requirements, while columns remained adequate due to higher initial safety factors. The structure was then modeled with four confinement reinforcement scenarios, varying stirrup quantity and spacing, to reflect typical field practices. Shear strength validation was conducted beforehand to ensure plastic mechanisms could form without premature shear failure. Nonlinear pushover analysis using SAP2000, supported by moment-curvature results from XTRACT, focused on (1) base shear and drift capacity, (2) plastic hinge formation, and (3) energy dissipation capacity. While all models satisfied Life Safety (LS) criteria, Model D-with the widest stirrup spacing-showed early stiffness degradation, exceeded shear capacity in some columns, and recorded the lowest energy dissipation. These results confirm the key role of proper stirrup detailing in enhancing strength, ductility, and seismic resilience.

Keywords: detailing deficiency, energy dissipation, performance-based design, pushover analysis, seismic performance.

Manuscript Received 9 September 2025; Revised 5 January 2026; Published 20 January 2026

INTRODUCTION

Indonesia's geographical location, surrounded by active tectonic plates and volcanic mountains, makes it highly susceptible to frequent earthquakes. One of the major earthquakes that occurred was in West Sumatra Province, specifically in the city of Padang. Padang, the provincial capital, is located on the western part of Sumatra Island. The city experienced a powerful earthquake on September 30, 2009, with a moment magnitude (Mw) of 7.5. The epicenter was 60 kilometers northwest of Padang, with a focal depth of 81 kilometers. Based on field observations, most of the damaged buildings and even collapsed buildings were frame buildings with unreinforced brick infill panels, some were unreinforced masonry, and a few were steel building structures (Bothara *et al.*, 2010). To reduce the risk from earthquakes, the government has made efforts to mitigate the damage and even collapse that can occur to buildings during an earthquake, especially in the aspect of structural design. As part of the first steps before the earthquake, the government has revised the structural design regulations three times in the last 20 years (Nugroho *et al*., 2022). The current design standard, especially for earthquake loading, is SNI 1726 2019, which is an update of SNI 1726 2012. Some changes that will significantly affect the design results of buildings designed with the old code are the increase in the value of the spectral response parameter (Faizah & Amaliah, 2021); (Salim & Sidi, 2024).

Unfortunately, the efforts made by the government are not followed by a good construction process. There are often differences between the results of the structural design, as set out in planning documents, such as technical specifications and detailed design engineering (DED), and what happens during the construction process. The results of research conducted in Padang City (West Sumatera Province) on the implementation of earthquake-resistant building standards, based on detailed design engineering (DED), found that the implementation of earthquake-resistant building standards is still low. With results ranging from 40,54 to 62,16 percent (Prihantony *et al*., 2020). It is also observed that no significant improvement in the period 2010-2019, after the major earthquake in Padang City, in terms of preventing casualties due to earthquake loads (Wardi *et al.*, 2018).

As one of the cities with high earthquake intensity, the special moment frame (SMF) is considered the most appropriate structural system for buildings in Padang City. In the context of earthquake-resistant building design, SMF has several requirements that must be fulfilled. Buildings are expected to perform well when subjected to design-level or major earthquakes. Key principles include the strong column weak beam concept, the collapse of the structural system must be dominant in the ductile mode, shear collapse is not allowed, the structure must be able to deform in elastically to achieve the desired performance, and avoid brittle pattern collapse (Moehle & Hooper, 2016). Although this system demands ductile structural performance, actual design practice generally still relies on a strength-based design approach (Yalçın *et al.,* 2021); (Suwondo & Arief, 2023), and structural analysis commonly adopts a linear elastic

method. In reality, the response of the structure to earthquake loads should be non-linear. To reflect the effect of non-linearity in the analysis of the structure, modifications are made by applying a structural modification factor, which reflects the expected ductility and energy dissipation capacity of the structure (Oggu *et al*., 2021).

In addition, applying response modification factors can reduce the design-level earthquake loads, resulting in a more economical cross-sectional design without compromising structural stability (Chiluka & Oggu, 2023). However, the impact of this reduction in earthquake load is the strictness of the limitations imposed on the detailing aspect. Detailing is expected to ensure that the structure performs well during an earthquake. However, in field practice, detailing factors are often not implemented according to standards. In various earthquake events, structural failures are often caused by non-compliance in the planning and implementation of buildings regarding the detailing aspect (Vafaei *et al*., 2019). In fact, many studies show that structures that do not meet detailing requirements tend to perform poorly during earthquakes. Some common mistakes include the use of plain reinforcement for shear reinforcement, insufficient confinement reinforcement in columns, excessive shear spacing, incorrect splicing locations, non-standard joint lengths, and poor connections at beam and column joints (Yön *et al*., 2024). Several studies show that applying confinement requirements, especially in beam and column elements, can increase the ductility of moment-bearing frame structures, even if the structures are not designed for earthquake loads (Vafaei & Alih, 2015). On the other hand, the lack of confinement reinforcement and the width of the spacing of the restraint reinforcement can reduce the structure's ductility (Antonius & Imran, 2012). It can even trigger premature collapse of the columns.

Numerous previous studies have numerically evaluated structural performance under earthquake loads using nonlinear static and dynamic methods. However, the specific impact of the amount and spacing of confinement reinforcement on the performance of structures, especially those built under older code provisions, has not been widely studied. Although some studies have addressed confinement, limited attention has been given to legacy buildings under revised seismic demands, particularly regarding detailed spacing and configuration. Moreover, these analyses often lack verification of the actual shear capacity based on the transverse reinforcement installed in the field, particularly in relation to the increased shear demand that arises during nonlinear analysis. To the best of the authors' knowledge, few studies validate whether as-built shear reinforcement remains sufficient under nonlinear demands. If the as-built shear capacity is exceeded, plastic hinges may not form as intended, and shear failure may govern the collapse mechanism. Consequently, the failure mechanism will not align with the intended ductile design but may instead lead to brittle collapse. Field observations have repeatedly shown that most collapsed buildings show no signs of flexural failure nor any development of global ductility before collapse (Pardalopoulos *et al*., 2022). Therefore, this study also highlights the importance of verifying the element's shear capacity before assessing other structural performance parameters. Thus, verifying shear capacity is not optional but fundamental for a comprehensive seismic performance evaluation.

To address this critical issue, a focused investigation is required to quantify how confinement detailing influences structural performance, particularly when legacy buildings are reassessed under updated seismic demands. This study aims to evaluate the effect of variations in confinement reinforcement, specifically the number of legs and transverse spacing, on the seismic performance of reinforced concrete buildings designed under previous regulations. The evaluation refers to the new provisions of SNI 1726:2019, beginning with an assessment of structural strength. Structural performance is examined nonlinearly using the pushover analysis method, focusing on base shear, drift capacity, plastic hinge formation, and energy dissipation. Before this, the shear capacity of the as-built transverse reinforcement is verified to ensure the plastic mechanism can form as intended. The findings of this study are expected to provide insights for improving detailing practices in legacy buildings under revised seismic codes.

LITERATUR REVIEW

Performance-Based Design is a method in which structural criteria are established to achieve specific performance objectives during a major earthquake (ATC40). The primary goal of this structural performance is to ensure that the displacements of the structure and its elements remain within acceptable limits under the considered seismic load. The performance level of a structure can be determined by identifying the extent of damage through direct observation of the structure during a design earthquake or even a major earthquake. This indicates a direct correlation between the cost of structural repairs and the severity of the damage, without disregarding the safety of the occupants (Wijaya *et al.*, 2019) . In addition to the measurable level of damage used as a basis for determining the structural performance level, the magnitude of the predicted seismic load also has a similar impact. This seismic load magnitude depends on the probability of an earthquake occurring within a specific return period (Ghobarah, 2001).

The static pushover analysis method is a technique that applies horizontal loads following the lateral deformation pattern of the dominant mode. The lateral load is gradually increased until the structure reaches its capacity limit. During this load increment process, the structural resistance condition is periodically updated to evaluate the level of damage, such as the formation of plastic hinges, that has occurred (Elnashai, 2001). This method can be applied under the condition

that the first lateral mode in both orthogonal directions has a significant dominance over other modes, with a contribution exceeding 75% (Budiono *et al*., 2016). The performance level of a structure is determined by identifying the intersection point between the capacity curve, which represents the structural capacity (the curve showing the relationship between force and maximum inelastic deformation), and the demand response spectrum curve. The methods used to generate these curves include the Capacity Response Spectrum method (ATC 40), the Displacement Method (FEMA 356), and the Displacement Modification Method (FEMA 440).

Structural performance is evaluated at both the global and local levels. For the local performance assessment, the acceptance criteria are based on rotational deformation limits as specified in ASCE 41-17 Figure-1. At the Immediate Occupancy (IO) performance level, the maximum allowable rotation shall not exceed 0.67 times the deformation limit defined for the Life Safety (LS) level. For the LS level, the maximum allowable rotation is limited to 0.75 of the rotation corresponding to point C on the moment-rotation curve. Meanwhile, for the Collapse Prevention (CP) level, the deformation limit corresponds to point E on the curve. The global structural performance is assessed by comparing the roof drift ratio against the allowable limits defined in FEMA 356 and FEMA 440. The loading method uses a displacement-controlled approach, with a target displacement value of 2% of the total building height, equivalent to 280 mm. To evaluate the structural performance, the performance point of the structure is determined.

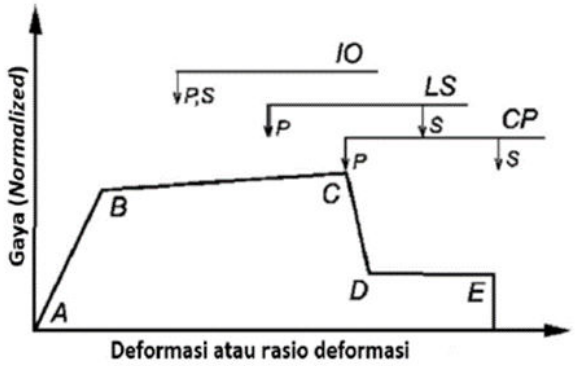

Figure-1. Illustration of acceptance criteria (ASCE/SEI) 41-17.

One of the approaches employed to determine the target displacement in the pushover analysis is the Displacement Modification Method. This method refers to FEMA 440-2005, which is an enhancement of FEMA 356-2000. The procedure involves modifying the linear elastic response of an equivalent Single Degree of Freedom (SDOF) system using modification factors C0, C1, C2, and C3, which result in the maximum global displacement (both elastic and inelastic), referred to as the target displacement (δt). The target displacement (δt) can be calculated using Equation (1), where C0 is the shape factor coefficient, C1 is the modification factor for the structural system conditions, C2 accounts for pinching effects, and C3 accounts for the amplification of lateral displacement due to the P-delta effect. In addition, Sa represents the spectral response acceleration, Te is the effective fundamental period of the structure, and g is the gravitational acceleration. This study adopts the Basic Safety Earthquake 1 for New Buildings (BSE-1N) as the seismic hazard level, which is defined as two-thirds of the Maximum Considered Earthquake (MCER). According to ASCE 41-17, the target seismic performance objective for office buildings classified under Risk Category II at the BSE-1N hazard level is Life Safety (LS). Accordingly, the structural analysis in this study was designed to evaluate whether the building meets the LS performance level when subjected to seismic demands equivalent to BSE-1N.

$$\delta t = C_o\, C_1\, C_2\, C_3\, S_a\, (Te/2\pi)^2\, g \quad (1)$$

METHODOLOGY

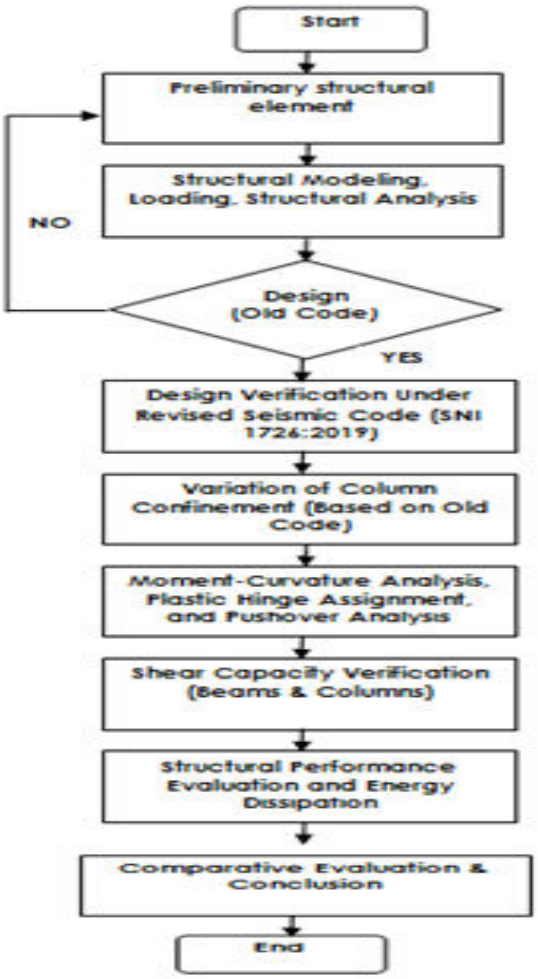

Figure-2. Research methodology flowchart.

Figure-2 illustrates the research methodology flowchart, providing a concise and visual representation of

the research steps undertaken in this study. The methodology outlines the sequential process of evaluating the seismic performance of reinforced concrete structures, with a particular emphasis on variations in the quantity and spacing of confinement reinforcement and their impact on overall structural performance.

Building Description

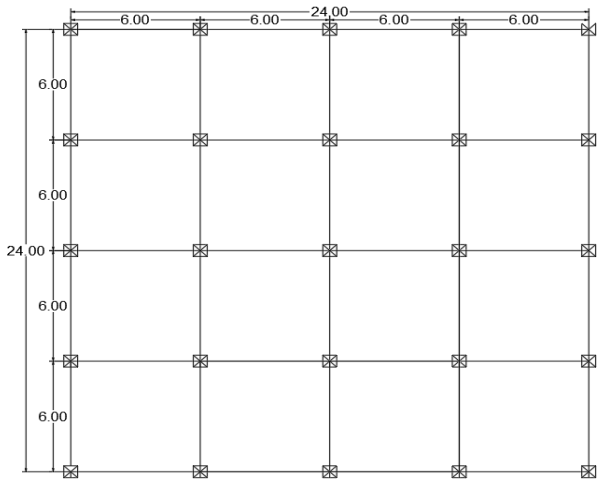

Figure-3. Structural Layout Plan.

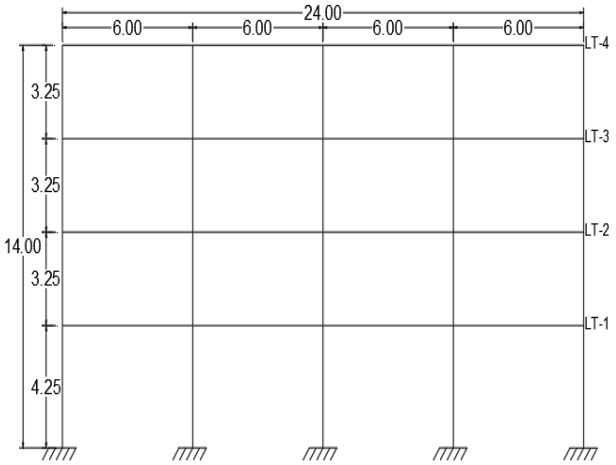

Figure-4. Structural elevation view.

In this study, the building to be analyzed and its performance evaluated is a low-rise building consisting of four levels. The building was designed using SNI 1726:2012 and SNI 2847:2013, as a sign that it was planned after the 2009 earthquake, whereas the regulations applicable at the time of the earthquake were SNI 1726:2002 and SNI 2847:2002. The building functions as an office building with Risk Category II and is built on medium soil. The building is classified under Seismic Design Category D. One of the structural system options used is a Special Moment Resisting Frame (SMRF). Meanwhile, the building has a square floor plan with dimensions of 24 × 24 meters. The spacing between columns is 6 m, with the height of the first-floor columns being 4.25 m, and the height between floors from the second floor to the roof is 3.25 m. The floor plan and structural sections can be seen in Figure-3 and Figure-4.

Structural Modeling, Loading, and Design

The dimensions of the main beams are determined to be 500 x 250 mm, while the secondary beams are 350 x 250 mm. The thickness of the floor slabs is specified as 130 mm for the second to third floors and 120 mm for the roof floor. Additionally, the columns are designed with uniform dimensions of 600 x 600 mm from the first to the fourth floor. The structural loads consist of dead loads, live loads, and earthquakes. Dead loads include the self-weight of the structure, calculated based on the unit weight of reinforced concrete (24 kN/m³) and the volume of structural elements. Additional superimposed dead loads are also considered, with values of 1.5 kN/m² for the first to third floors and 1.0 kN/m² for the roof floor. These additional loads account for plastering, tiles, ceilings, as well as mechanical and electrical installations. Furthermore, there is a perimeter brick wall load with a weight of 2.5 kN/m². The live loads for an office building are 3.12 kN/m² for the first to third floors and 1.0 kN/m² for the roof floor. The most critical load is the earthquake load, which is derived from the seismic map specified in SNI 1726:2012. For Padang City, classified as a soft soil site (SD), the seismic parameters are as follows: Ss = 1.1245 g, S1 = 0.5737 g, SDS = 0.750 g, and SD1 = 0.790 g. Subsequently, the structure is modeled and analyzed using SAP2000 software. In the modeling process, columns and beams are represented as frame elements, while floor slabs are modeled as shell elements. Regarding material properties, the concrete used has a compressive strength (fc) of 25 MPa. For the reinforcement steel, the yield strength (fy) is 420 MPa, and the ultimate strength (fu) is 550 MPa.

Based on the results of linear static and dynamic analyses, followed by structural design, the final cross-sectional configuration of the structural elements is determined as follows. Beams are reinforced with 3D25 bars at the top and 2D25 bars at the bottom, with 2D10-100 stirrups provided in the support regions and 2D10-200 in the spans. Columns use 12D22 longitudinal bars, yielding a reinforcement ratio of 1.29%, while confinement reinforcement consists of 4D13-150 stirrups. All elements satisfy design requirements based on SNI 2847 2013, including minimum reinforcement ratios and the Strong Column–Weak Beam (SCWB) principle. The final design configuration is illustrated in Figure-5.

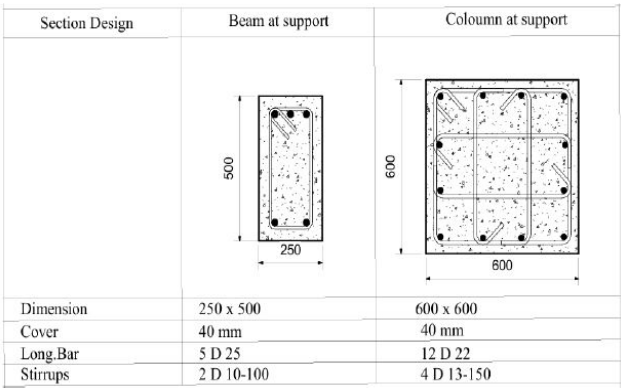

Dimension	250 x 500	600 x 600
Cover	40 mm	40 mm
Long.Bar	5 D 25	12 D 22
Stirrups	2 D 10-100	4 D 13-150

Figure-5. Cross-sectional details of the beam and column elements at the support.

Definition of Scenario

To assess the impact of discrepancies in confinement reinforcement on the columns regarding the performance level of structures designed based on SNI 2847:2013 and SNI 1726:2012, four structural modeling scenarios were developed. Model A was designed in full compliance with the regulations and met all the requirements for the Special Moment-Resisting Frame System (SMRF). In Model B, the confinement reinforcement in the columns was reduced to 75% of the prescribed amount. Model C employed only 50% of the required confinement reinforcement, while maintaining the original spacing of stirrups. Model D employed the same 50% confinement reinforcement as Model C, but with an increased stirrup spacing of 300 mm, effectively doubling the spacing used in Model A. For a detailed overview of each model, refer to Table-1. Each model's performance will be evaluated to determine the impact of confinement reinforcement discrepancies on structural performance, using the current seismic load standards in Indonesia, namely SNI 1726:2019. These confinement configurations were selected to reflect typical stirrup detailing conditions commonly found in reinforced concrete buildings constructed in Indonesia, especially those constructed before the adoption of modern seismic design codes.

Table-1. Column confinement variations for Models A-D.

Model	dt (mm)	leg	s (mm)	fy (MPa)
A	13	4	150	420
B	13	3	150	420
C	13	2	150	420
D	13	2	300	420

Nonlinear Analysis Setup and Development of Moment-Rotation Curves

The first step in nonlinear analysis involves modeling the potential plastic hinges that may form in beams and columns. The analysis begins by defining the material properties under nonlinear conditions. Materials are categorized into three types: (1) the concrete cover, assumed to be unconfined concrete, (2) the core concrete, modeled as confined concrete, and (3) the reinforcing steel. The confined concrete is modeled based on the principles and equations of the Mander model, while the reinforcing steel follows the typical stress-strain behavior of reinforcing bars. Subsequently, sectional-level analysis is conducted through moment-curvature analysis. For beams, the applied load induces flexural moment along the major axis (M3), whereas for columns, there is an interaction between moment and axial force. The axial load considered in the moment-curvature analysis is the combination of Dead Load, Superimposed Dead Load, and 0.25 Live Load. In this study, particular emphasis is placed on the columns. Four moment-curvature models are developed based on the design configurations presented in the corresponding Table-1. After modeling using the XTRACT software, key parameters-such as yield moment, yield curvature, ultimate moment, and ultimate curvature are obtained for each cross-section analyzed, both for beams and columns.

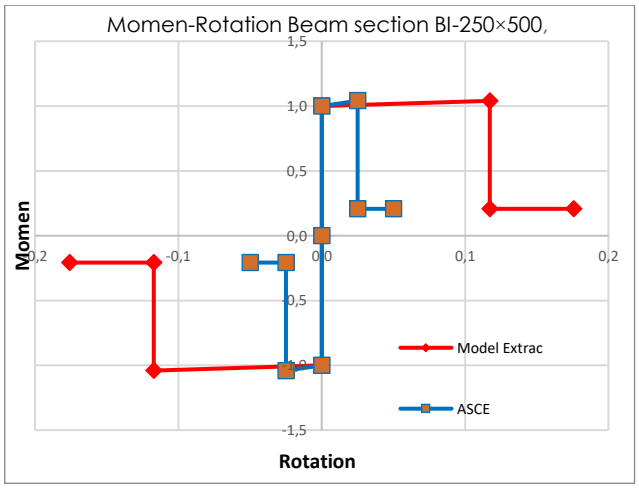

Figure-6. Moment-rotation of the Beam section.

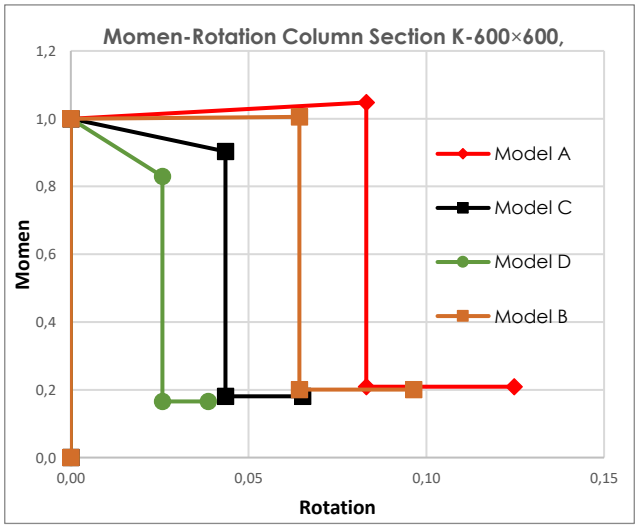

Figure-7. Moment-rotation of Column section.

The rotation value is determined by multiplying the curvature by the plastic hinge length of each structural element. The plastic hinge length is calculated based on the provisions of SNI 2847:2019, which state that the length of the frame element expected to yield in flexure due to design-level earthquake displacement must be extended by at least h from the critical section-defined as the initial location of flexural yielding. In addition to the numerical approach using XTRACT, the moment-rotation backbone curve is also developed based on empirical methods recommended by ASCE 41-17. For beam elements, the moment-rotation values used in structural modeling are conservatively selected as the minimum between the ASCE 41-17 based empirical values and the numerical results obtained from XTRACT. For column elements, given that this study focuses on evaluating the influence of confinement variation on structural performance, the backbone curves are entirely derived from the numerical analysis conducted using XTRACT. Figure-6 and Figure-7 present the resulting moment-rotation curves for beam and column elements, respectively. From the comparison of backbone curves, it can be concluded that beam elements adopt empirical backbone curves (ASCE 41 tables), while column elements use backbone curves obtained from numerical modeling (XTRACT) (Imran *et al*., 2024). The Stiffness Degrading Takeda Model is applied as the hysteretic behavior model for all nonlinear element parameters throughout the structural system.

RESULTS AND DISCUSSIONS

Design Verification Under Revised Seismic Code (SNI 1726:2019)

The revision of seismic load regulations from SNI 1726 2012 to SNI 1726 2019 has resulted in a significant increase in base shear demand. Based on structural analysis using the equivalent static method, a 13.33% increase in seismic load was observed, raising the total base shear to 2556 kN. This change inevitably led to increased internal forces throughout the structure. Specifically for beam elements, the maximum moment at the top support increased to Mu = 224.39 kNm, representing a 17.60% rise compared to the previous design. Under the original reinforcement configuration, it was found that the flexural capacity (longitudinal reinforcement) no longer satisfies the strength requirements, as the previously calculated design strength was only ØMn = 211 kNm. The increase in moment due to the application of new earthquake loads (SNI 2019) indicates that existing beam elements require special attention, including potential strengthening or retrofitting.
The increase in internal forces also occurred in the column elements, but their strength capacity still met the design requirements. This was due to the use of a relatively high safety factor in the design according to previous regulations. The stress ratio used was relatively high, with a value of 1.565. The high stress ratio value was influenced by the SCWB requirements that must be met, where the column was designed to be stronger than the beam, so the column strength must be greater than the beam strength (Ghorbanzadeh & Khoshnoudian, 2022). The impact of the increase in internal forces due to increased earthquake parameters on the structure is reflected in the reduction in the safety factor value, namely from 1.565 to 1.123, as shown in Table-2.

Table-2. Demand-to-Capacity Ratio of Column.

No	Mux	Muy	Phi (Mnx)	Phi (Mny)	Phi(Mn)/ Mu
	kNm	kNm	kNm	kNm	
1	-2.04	2.04	-363.17	363.17	177.93
2	-4.31	104.6	-18.07	438.47	4.192
3	-515.5	-116.52	-580.12	-131.13	1.125
4	515.5	120.64	578.87	135.47	1.123
5	-116.52	-515.5	-131.13	-580.12	1.125
6	120.64	515.5	135.47	578.87	1.123

Assessment of Brittle Failure Potential Through Shear Analysis

Before assessing the structural performance level, it is essential to verify that brittle failures do not occur in the beam and column elements, particularly in regions expected to undergo plastic hinging. To ensure that plastification develops as intended, shear failure must be prevented in these regions by ensuring that their shear strength exceeds the corresponding shear demands, thus remaining elastic during the nonlinear pushover analysis. To evaluate the potential for brittle failure mechanisms, a comparison was conducted between the shear demand and the nominal shear capacity of all beam and column elements across the four confinement models. The shear

demand was obtained from internal force results at the performance point, representing the stage where the structure reaches its target displacement under pushover loading. This evaluation confirms whether the assigned plastic hinges can form properly without being preceded by shear failure.

Table-3. Shear Safety Assessment Based on the Ratio of Shear Strength to Shear Demand (ØVn/Vu).

Model	Balok		Kolom	
	ØVn / Vu	Cek	ØVn / Vu	Cek
A	1.21	OKE	2.209	OKE
B	1.21	OKE	1.675	OKE
C	1.22	OKE	1.334	OKE
D	1.25	OKE	0.981	NOT OKE

Table-3 illustrates a comparison between the nominal shear capacities of beam and column elements based on four installation scenarios, with the maximum shear force occurring when the structure reaches its performance point. In the beam elements, no shear failure occurred despite a significant increase in internal forces during the pushover analysis. This is indicated by the capacity-to-demand ratio for all four models reaching approximately 1,2. Meanwhile, for columns, there was significant variation within each model, with ratio values ranging from 0,981 to 2,209. Unlike beams, for which no variation in the amount of confinement reinforcement was used in this study, the reduction in the amount of confinement was significant, with a significant decrease in the ratio. It was also noted that column model D had a ratio that did not meet the requirements, with a value of less than 1. This poses a risk of shear failure before flexural plastification develops, which could defeat the plastic hinge mechanism and lead to brittle failure. Model D represents the most minimal confinement conditions (e.g., a small number of stirrups and large spacing), thus directly demonstrating the significant effect of confinement detailing on column shear capacity. These results emphasize that before evaluating a structure's performance nonlinearly (e.g., with pushover), it is necessary to verify the shear capacity to avoid brittle failure that could misinterpret the structure's performance.

Nonlinear Pushover Analysis Result

Figure-8 is a graph of the relationship between base shear and displacement that occurs based on the results of the pushover analysis. Among the four models, it is known that Model A, which is the model that complies with the standard, has the highest base shear capacity compared to the other three models. The decrease in shear force is in line with the reduction of confinement reinforcement and the increase in the spacing of the transverse reinforcement provided. In line with the results of the shear capacity check, Model D is the model with the worst stiffness degradation among the four models. This indicates that Model D shows potential failure, because its previous shear strength did not meet the requirements, making it difficult to develop an optimal plastic hinge mechanism.

Furthermore, Models C and D began to lose stiffness earlier, as seen from the curves that started to flatten when the displacement reached around 150 mm. In addition, the graph also shows that after the displacement of 100 mm, there is an increasingly clear difference between the models. This indicates that confinement reinforcement plays a significant role in the inelastic zone. Meanwhile, based on the data in Table-4, the performance of each model can be determined. The analysis results show that all four models fall into the Life Safety (LS) category with drift ratios between 1.93% and 1.95%. FEMA 440 requires that the maximum permissible drift for the Life Safety category be 2%. Although differences in the moment-curvature response of the four models are observed, as shown in Figure-7, the analysis results indicate that the structural performance is not significantly affected. Consistent with previous studies by (Bilgin & Plaku, 2024), the variations in the moment-curvature response of column cross-sections do not have a substantial impact on the overall performance of the system.

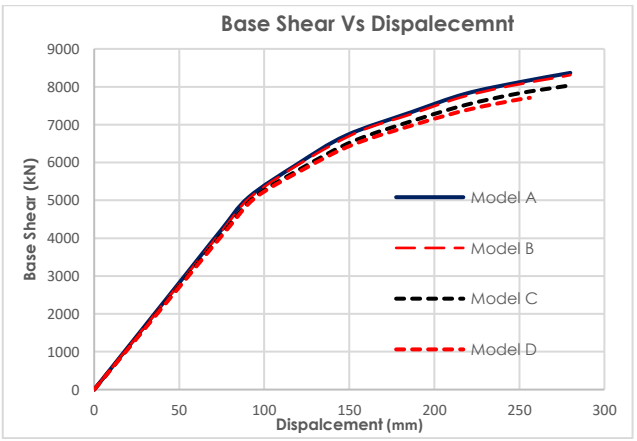

Figure-8. Base shear vs Displacement.

Table-4. Performance Drift Ratio Calculation.

Model	Performance Point		drift (%)
	V (kN)	D (mm)	
A	8297.02	272	1.943
B	8252.268	273	1.950
C	7966.192	270	1.929
D	7708.339	270	1.929

Formation of Plastic Hinges

To evaluate the progression of inelastic behavior under lateral loading, the formation of plastic hinges at

various performance levels was closely monitored throughout the pushover analysis. The transition of hinges from initial yielding (B to IO), through intermediate damage states (IO to LS), and into critical deformation zones (C) to (CP). Table-5 summarizes the key parameters for each confinement model, including the load step, base shear, and displacement at which plasticity first occurred, along with the number of elements reaching each performance level.

Table-5. Plastic Hinges Development Summary at Different Performance Levels.

(a) First Occurrence of Plastic Hinges (B to IO)

Model	Step	Displacement (mm)	Base Shear (kN)
A	3	75	4230.50
B	3	76	4253.04
C	3	78	4258.48
D	3	79	4259.00

(b) Intermediate Plastic Hinges (IO to LS)

Model	Step	Displacement (mm)	Number of Hinges (n)
A	8	218	24
B	8	216	20
C	8	219	29
D	9	220	34

(c) Severe Plastic Hinges (C to CP)

Model	Step	Displacement (mm)	Number of Hinges (n)
A	10	280	2
B	10	280	4
C	10	280	5
D	10	256	7

All models exhibited their first yielding at Step 3, with base shear values ranging from 4230 to 4259 kN, indicating consistent initial stiffness across all designs. A comparison between the code-prescribed elastic design base shear and the nonlinear pushover results reveals a considerable inherent strength reserve in the structural system. The elastic base shear according to SNI 1726 2012 was 2256.08 kN and increased to 2556 kN under SNI 1726 2019, reflecting a 13.33% rise due to updated seismic load requirements. In contrast, the base shear corresponding to the onset of yielding was significantly higher, ranging from 4230 to 4259 kN. This represents a strength reserve of approximately 66-89% above the elastic design shear, underscoring the structure's ability to resist seismic forces beyond code-level provisions before entering nonlinear behavior. These findings further highlight the importance of performance-based design approaches, as code-based elastic analysis may underestimate both the available strength and the critical role of post-yield behavior in ensuring structural safety.

Although all models exhibited similar stiffness and base shear capacity during the early elastic stage-evidenced by the simultaneous emergence of B to IO hinges at Step 3-the influence of transverse confinement detailing became increasingly pronounced in the inelastic range. This distinction is clearly illustrated in the IO to LS and especially in the C to CP performance zones. Notably, Model D, which employed the weakest confinement configuration, exhibited the highest number of plastic hinges in both categories, along with the lowest base shear at the final displacement step. This reflects a premature loss in lateral load resistance and suggests that insufficient confinement accelerates stiffness degradation while limiting the structure's capacity to sustain ductility under increasing lateral demands. The severe hinge formation in the C to CP zone particularly underscores this effect. While Model A formed only two plastic hinges in this critical range, Model D developed as many as seven, accompanied by a reduced maximum displacement (256 mm compared to 280 mm).

This trend reinforces the conclusion that effective confinement plays a vital role not in initial stiffness, but in post-yield performance, energy dissipation, and damage limitation during severe nonlinear deformation. The formation and distribution of plastic hinges provide direct insight into the structural response under seismic loading. The early hinge formation confirms comparable initial stiffness, while divergence in the IO to LS and C to CP stages highlights the importance of confinement in maintaining structural integrity beyond the elastic threshold. These findings affirm that inadequate detailing leads to earlier and more extensive plasticity, particularly in critical performance zones, thereby validating the strong correlation between transverse reinforcement and structural resilience.

Energy Dissipation

Based on the law of conservation of energy, incoming earthquake energy is not destroyed but is converted into elastic and plastic deformations, and some is absorbed as dissipative energy, as discussed in previous studies (Karaka & Tripathi, 2023). Dissipative energy reflects a structure's ability to absorb earthquake loads through stable plastic deformation. In pushover analysis, the amount of dissipative energy is calculated from the area of the base shear and displacement curve, which indicates the total energy absorbed by the structure during nonlinear deformation. This shows that the greater the energy that can be dissipated, the higher the resistance of the structure to the acting earthquake load.

Based on Figure-9, it is known that Model A-as the model with the best detailing-has the largest dissipation energy, which is 1582.09 kN·m. This value continues to decrease until it reaches 1320.42 kN·m in Model D, with a decrease difference of 17% compared to

Model A. The decrease in dissipation energy in Model D shows that inadequate confinement detailing has a direct impact on the structure's ability to absorb earthquake energy. In addition, the closer the distance between the stirrups, the greater the energy that can be dissipated. This condition will delay the occurrence of stiffness degradation and maintain the stability of the structure in large inelastic deformation.

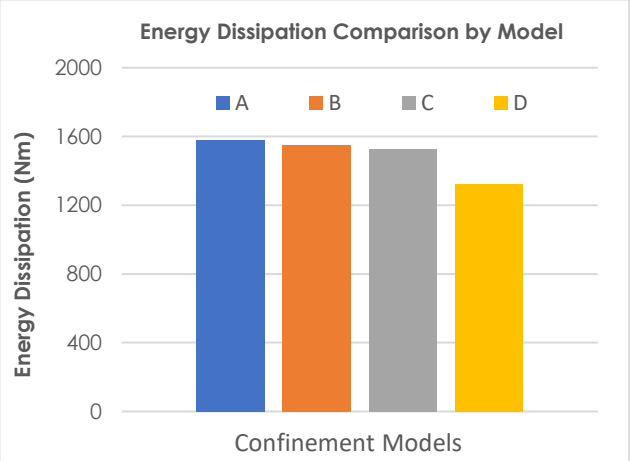

Figure-9. Energy Dissipation Per Model.

CONCLUSIONS

This study shows that although building structures designed based on SNI 2012 are generally still able to meet the Life Safety performance limits based on drift and base shear evaluations according to SNI 1726:2019, there are potential failure modes if the confinement detailing is insufficient. In addition, this study also investigates the effect of shear reinforcement detailing on the performance of reinforced concrete buildings using non-linear static analysis. Four confinement models (A-D) are compared, which represent variations in the number of confinement reinforcement and reinforcement spacing. The structural performance evaluation includes shear strength when the performance point is reached, structural performance categories, plastic hinge formation, and dissipated energy.

The analysis results show that variations in the number of legs and stirrup spacing significantly affect the shear capacity, plastic hinge formation sequence, and dissipation energy in the structure. The model with the least stirrup detailing (Model D) showed that the column shear capacity was not met (ratio < 1) during the pushover analysis, while for structural performance, the results showed that although the overall structural performance in terms of drift ratio remained within the Life Safety (LS) category limits, namely between 1.93%-1.95%. Model A, which has the most complete transverse reinforcement configuration, consistently showed the best performance in all aspects-achieving the highest base shear value (8297.02 kN), the fewest number of heavy plastic hinges, and the highest dissipation energy (1582.09 kN m). In contrast, Model D, which has the least level of confinement, showed earlier stiffness degradation, the shear forces that occurred during the pushover analysis exceeded the shear capacity of the column, and recorded the lowest dissipation energy, indicating lower structural resistance to large earthquake loads.

In conclusion, this study confirms that confinement detailing directly affects a structure's ability to maintain strength, delay stiffness degradation, and dissipate energy during seismic loading. While all models met the Life Safety performance targets, improving the stirrup configuration-particularly in terms of stirrup spacing-can significantly improve the structure's seismic resistance.

Acknowledgements

This work was supported by the Penelitian Dasar (PD) research scheme with contract number 1802/UN35.15/LT/2024, provided by the Institute of Research and Community Service (LPPM), Universitas Negeri Padang, Indonesia.

REFERENCES

Antonius and Imran I. 2012. Experimental study of confined low-, medium-, and high-strength concrete subjected to concentric compression. ITB Journal of Engineering Science, 44 B(3): 252-269. https://doi.org/10.5614/itbj.eng.sci.2012.44.3.4

Bilgin H. and Plaku B. 2024. Influence of Confined Concrete Models on the Seismic Response of RC Frames. SDHM Structural Durability and Health Monitoring, 18(3): 197-222. https://doi.org/10.32604/sdhm.2024.048645

Bothara J., Beetham D., Brunsdon D., Brown R., Hyland C., Lewis W., Miller S., Sanders R. and Sulistio Y. 2010. General observations of effects of the 30th September 2009 Padang Earthquake, Indonesia General Observations of Effects of the 30th September 2009 Padang Earthquake, Indonesia. August 2016. https://doi.org/10.5459/bnzsee.43.3.143-173

Budiono B., Wicaksono E. B., Teoretis J., Bidang T., Sipil R., Terapan D., Rekayasa B. and Abstrak S. 2016. Perilaku Struktur Bangunan dengan Ketidakberaturan Vertikal Tingkat Lunak Berlebihan dan Massa Terhadap Beban Gempa. Jurnal Teknik Sipil Institut Teknologi Bandung, 23(2). https://doi.org/https://doi.org/10.5614/jts.2016.23.2.4

Chiluka S. and Oggu P. 2023. Performance Assessment of Ductile Detailing Code-Based Reinforced Concrete Special Moment-Resisting Frames. International Journal of Engineering, Transactions A: Basics, 36(3): 457-464. https://doi.org/10.5829/ije.2023.36.03c.04

Elnashai A. S. 2001. Advanced inelastic static (pushover) analysis for earthquake applications. In Structural Engineering and Mechanics (12(1): 51-69). Techno-Press. https://doi.org/10.12989/sem.2001.12.1.051

Faizah R. and Amaliah R. 2021. Comparative Study of Indonesian Spectra Response Parameters for Buildings According To 2012 and 2019 Seismic Codes. International Journal of Integrated Engineering, 13(3): 168-175. https://doi.org/10.30880/ijie.2021.13.03.020

Ghobarah A. 2001. Performance-based design in earthquake engineering: State of development. Engineering Structures, 23(8): 878-884. https://doi.org/10.1016/S0141-0296(01)00036-0

Ghorbanzadeh M. and Khoshnoudian F. 2022. The Effect of Strong Column-Weak Beam Ratio on the Collapse Behaviour of Reinforced Concrete Moment Frames Subjected to Near-Field Earthquakes. Journal of Earthquake Engineering, 26(8): 4030-4053. https://doi.org/10.1080/13632469.2020.1822228

Imran I., Siringoringo D. M. and Rainayana S. S. 2024. Seismic evaluation and retrofit of a typical reinforced concrete hospital building in Indonesia with DCFP isolation system. Structures, 64. https://doi.org/10.1016/j.istruc.2024.106593

Karaka, H. K. and Tripathi, R. K. 2023. Assessing potential damage and energy dissipation in low-rise high-strength concrete frames with strong infill walls using the applied element method. Innovative Infrastructure Solutions, 8(11). https://doi.org/10.1007/s41062-023-01283-7

Moehle J. P. and Hooper J. D. 2016. Seismic Design of Reinforced Concrete Special Moment Frames: A Guide for Practicing Engineers, Second Edition. NEHRP Seismic Design Technical Brief No. 1, 2, 27. http://nehrp.gov/pdf/nistgcr8-917-1. pdf%0Ahttps://nvlpubs.nist.gov/nistpubs/gcr/2016/NIST. GCR.16-917-40.pdf

Nugroho W. O., Sagara A., and Imran I. 2022. The evolution of Indonesian seismic and concrete building codes: From the past to the present. Structures, 41, 1092-1108. https://doi.org/10.1016/j.istruc.2022.05.032

Oggu P., Gopikrishna K. and Nagariya A. 2021. Seismic behavior and response reduction factors for concrete moment-resisting frames. Bulletin of Earthquake Engineering, 19(13): 5643-5663. https://doi.org/10.1007/s10518-021-01184-z

Pardalopoulos S. I., Pantazopoulou S. J. and Manolis G. D. 2022. On the Modeling and Analysis of Brittle Failure in Existing R/C Structures Due to Seismic Loads. Applied Sciences (Switzerland), 12(3). https://doi.org/10.3390/app12031602

Prihantony D. I., Afrizal A., Hadiguna R. A. and Ophiyandri T. 2020. Penerapan Standar Bangunan Tahan Gempa Dalam Detailed Engineering Design Di Sumatera Barat. Jurnal Rekayasa Sipil (JRS-Unand), 16(3): 166. https://doi.org/10.25077/jrs.16.3.166-177.2020

Salim J. T. and Sidi I. D. 2024. Comparative Seismic Evaluation of Building Codes: A Case Study on Structural Performance and Safety. Journal of Engineering and Technological Sciences, 56(6): 793-807. https://doi.org/10.5614/j.eng.technol.sci.2024.56.6.10

Suwondo R., and Arief M. B. U. 2023. Evaluating the Seismic Performance of Low-Rise Concrete Buildings Using Nonlinear Static Analysis. Civil Engineering and Architecture, 11(4): 1976-1983. https://doi.org/10.13189/cea.2023.110422

Vafaei M. and Alih S. C. 2015. Seismic detailing, a compromised principal for seismic design in Malaysia. Proceedings of the APSEC & ACEC 2015, 342–347.

Vafaei M., Baniahmadi M. and Alih S. C. 2019. The relative importance of the strong column-weak beam design concept in the single-story RC frames. Engineering Structures, 185, 159-170. https://doi.org/10.1016/j.engstruct.2019.01.126

Wardi S., Sanada Y., Kita M., Tanjung J. and Maidiawati. 2018. Common structural details and deficiencies in Indonesian RC buildings: Preliminary report on field investigation in Padang City, West Sumatra. International Journal on Advanced Science, Engineering and Information Technology, 8(2): 418-425. https://doi.org/10.18517/ijaseit.8.2.4207

Wijaya U., Soegiarso R. and Tavio. 2019. Evaluation of seismic performance based on a direct displacement-based method. International Journal on Advanced Science, Engineering and Information Technology, 9(5): 1716-1724. https://doi.org/10.18517/ijaseit.9.5.7932

Yalçın C., Dindar A. A., Yüksel E., Özkaynak H. and Büyüköztürk O. 2021. Seismic design of RC frame structures based on the energy-balance method. Engineering Structures, 237(February). https://doi.org/10.1016/j.engstruct.2021.112220

Yön B., Dedeoğlu İ. Ö., Yetkin M., Erkek H. and Calayır Y. 2024. Evaluation of the seismic response of reinforced concrete buildings in the light of lessons learned from the February 6, 2023, Kahramanmaraş, Türkiye earthquake sequences. In Natural Hazards (Issue February 2023). https://doi.org/10.1007/s11069-024-06859-9